

A Monte Carlo Study on the Identification of Quark-gluon Fusion Product in QCD-instanton Induced Processes in Deep-inelastic Scattering

Xu Mingmei and Liu Lianshou*¹

¹*Institute of Particle Physics, Huazhong Normal University, Wuhan 430079, China*

Different methods to reconstruct the quark-gluon fusion product and current jet are tried in deep-inelastic e-p scattering events with instanton as background generated by QCDINS Monte Carlo code. A comparison of these methods are performed and a good method is found which can reconstruct well the energies of current jet and instanton product as well as the mass of the latter. The isotropy property of the instanton product and jet are calculated and compared. A parameter characterizing the degree of “hardness” of the instanton product is presented.

PACS numbers: 13.85.Hd; 13.60.-r; 05.45.Yv; 05.10.Ln

I. INTRODUCTION

In the Standard Model, both the strong and the electro-weak interactions are described by non-Abelian gauge theory. In these theories, the ground state has a rich topological structure, associated with non-perturbative fluctuations of the gauge field, called instantons [1, 2, 3, 4], which represent tunneling transition between topologically non-equivalent vacua. In the strong sector, described by QCD, instantons are non-perturbative fluctuations of the gluon field. Deep-inelastic scattering (DIS) offers a unique opportunity to discover the processes induced by QCD instantons. The rate is calculable within “instanton-perturbative theory” and is found to be sizable [5, 6, 7].

QCD-instanton induced process leads to a characteristic final state, which allows instanton induced events to be distinguished from the normal DIS processes. For a leading graph in QCD-instanton induced e-p collision, *cf.* Fig. 1, the incident lepton emits a photon, with 4-momentum q , which in turn transforms into a quark-antiquark pair. One of these quarks with 4-momentum q'' hadronizes to form the *current jet*. The other quark, with 4-momentum q' , fuses with a gluon (4-momentum g) from the proton in the presence of an instanton. The $q'g$ interaction is called the hard subprocess of photon-gluon-fusion process. For simplicity, we will in the following call the hadron system produced from the fusion of quark-gluon in the presence of an instanton as *instanton final state* (IFS).

The phenomenological characteristics of instanton induced events can be summarized as follows [8]:

- In the hard subprocess exactly one $q\bar{q}$ pair of each of the n_f kinematically accessible quark flavors participates in the hard subprocess of each event, either as incoming or as outgoing object. This feature is often termed as “flavour democracy”. The number of gluons emitted per event follows a Poisson distribution with average value $\langle n_g \rangle \sim O(1/\alpha_s) \sim 3$. The n_g

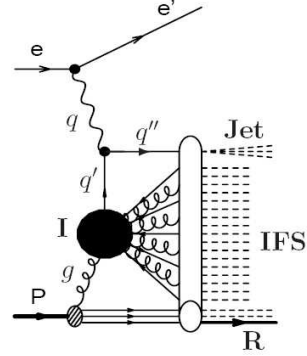


FIG. 1: The leading QCD-instanton induced process in the DIS regime of e-p scattering.

gluons plus $2n_f - 1$ outgoing (anti-)quarks give rise to a high multiplicity final state.

- The particles produced from the quark-gluon fusion in the presence of instanton, *i.e.* the IFS, are expected to be isotropically distributed in their center of mass frame.
- From theoretical point of view, the most prominent characteristic of instanton induced events, which is also the most difficult feature to be observed experimentally, is the *chirality violation*. In instanton induced events, all quarks produced in the hard subprocess are emitted with the same handedness, that means

$$\gamma^* + g \xrightarrow{I} \sum_{n_f} (q_R + \bar{q}_R) + n_g g, \quad (I \rightarrow \bar{I}, R \rightarrow L). \quad (1)$$

Although the existence of instanton is required by the Standard Model, the experimental evidence is still lacking. HERA offers a unique chance to discover instanton, which would be a confirmation of an essentially non-perturbative Standard Model prediction.

Two experiments, H1 and ZEUS, have reported their search for QCD-instanton induced processes in DIS at HERA [9, 13]. While an excess of events with instanton-like topology has been observed, it cannot

*Email: liuls@iopp.ccnu.edu.cn

be claimed significantly given the uncertainty of simulation and theory. Upper limits on the cross-section for instanton induced processes are set dependent on the kinematic domain considered.

One of the chief problems in instanton-searching is to identify the IFS, current jet and proton remnant. Only when the IFS and jet are identified precisely the reconstruction of the kinematic variables such as $Q'^2 \equiv -q'^2$, $x' \equiv Q'^2/(2g \cdot q')$ can be good and the discriminating variables for instanton-searching can be reliable.

At partonic level the separation of different parts is clear, *cf.* Fig. 1. The mother parton of current jet is the quark q'' . The “mother” of IFS is the quark q' and gluon g in the presence of I. The best identification of IFS and jet would be to minimize the differences between the energies and masses of IFS and current jet with those of their “mother” — $q' + g$ and q'' . However, this could be achieved only in Monte Carlo study but not in real experiment, because the 4-momenta at partonic level are unmeasurable.

Monte Carlo simulation has been applied to the problem in consideration by some authors [9, 10, 11, 12, 13, 14, 15]. Their main goal was concentrated on finding some methods that can be used in experiments, and the information at partonic level has been used only for evaluating the methods.

For jet finding, both the cone algorithm [9, 10, 11, 12] and the k_t -cluster algorithm [13, 14, 15] have been used. The cone size has been chosen to optimize the reconstruction of Q'^2 [10]. The IFS is identified by a pseudo-rapidity band with width 1.1, where the width is chosen for the expectation of an isotropic IFS in its rest frame. While the k_t algorithm has not done any optimization and the identification of IFS was through quadrant [14] according to its proper position. Although these methods play an important role in the present searching strategy, the optimization needs improving.

The aim of the present paper is to re-consider the Monte Carlo study of the problem and identify IFS through directly optimizing its energy and mass as well as the energy of current jet. The resulting IFS is of high precision and can be used in the theoretical study of instanton physics. The method used here is not directly applicable to real experiments but can provide instructions for the IFS identification in experimental study.

The layout of the paper is as follows. In Sec. II some information at the partonic level of the instanton induced events will be presented. Several new methods for the reconstruction of IFS in Monte Carlo simulation will be proposed and compared in Sec. III. A good method is found which can reconstruct well the energies of current jet and instanton as well as the mass of the latter. The isotropy property of the obtained IFS will be discussed in Sec. IV in comparison with that of the current jet. Sec. V is a summary.

II. BASIC DISTRIBUTIONS WITH PARTONIC INFORMATION

Our study is based on the Monte Carlo generator QCDINS [16, 17] for instanton induced events. It is a MC package to simulate quark-gluon fusion process $q' + g \xrightarrow{(I)} X$ in the background of instanton. It acts as a hard subprocess generator embedded in the HERWIG [18, 19] program. The subsequent fragmentation and hadronization are handled by HERWIG. In the following the default parameters of the QCDINS 2.0 version are used, i.e. $x' > 0.35$, $Q'^2 > 113 \text{ GeV}^2$ and the number of flavors is set to be $n_f = 3$.

Final states in instanton induced DIS consist of 4 subsystems: 1- scattered lepton, 2- hadrons from current quark, 3- hadrons created from the fusion of quark and gluon in the background of instanton (*instanton final state* for short), 4- proton remnant group of particles, *cf.* Fig. 1. The reconstruction is based on the assumption that the color forces among the current jet, the instanton part and the proton remnant are weak so that each part can be approximately separated and the momentum of hadronic final state of each part is approximately equal to those of the corresponding part at partonic level.

In HERWIG the scattered electron is easily identified by particle ID and status code. We discard it first. The particles left are the mixture of current jet (C for short), instanton final state (I for short) and proton remnant (R for short).

After rejecting the scattered lepton, all the objects in the hadronic final state are boosted to the hadronic center-of-mass frame (hcm). This frame is defined by $\mathbf{q} + \mathbf{P} = 0$, where \mathbf{q} and \mathbf{P} are the 3-momenta of the exchanged photon and proton, respectively. The positive Z -direction of hcm frame is defined in the direction of photon momentum. In the hcm frame, in order to see the jet signal, we remove the ϕ angle of current quark for every final state particles in every event. That means letting the ϕ angle of current quark equal 0 and hence the jet fragments are around $\phi = 0$. The 2D distributions of θ and ϕ for all final state particles are plotted in Fig.2. The 1D distribution of θ for all the final state particles is plotted in Fig.3 (a). Also plotted in Fig.3 (b)-(d) is the partonic information of C, I and R. The angle θ is measured against the direction of photon.

III. THREE METHODS FOR IFS IDENTIFICATION

Method 1: p_z -sorting

Fig. 3(a) illustrates that the final state particles distribute mainly around two back-to-back directions — $\theta = 0$ and π . Around $\theta = 0$ are C and the main part of I, around $\theta = \pi$ are R and a little I. The method to discard R in ZEUS experiment [13] is to do a $\theta = \frac{\pi}{2}$ cut, taking particles with $\theta^{\text{hcm}} > \frac{\pi}{2}$ as proton remnant. In fact, as can be seen from Fig.

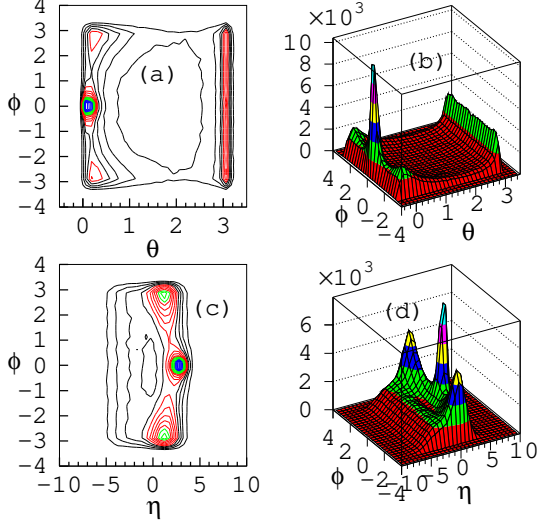


FIG. 2: (Color online) 2D plot in hcm after removing the ϕ angle of current quark. (a)(b) — ϕ vs. θ in contour and surface plots, respectively; (c)(d) — ϕ vs. η (η is defined as $-\log(\tan \frac{\theta}{2})$) in contour and surface plots, respectively.

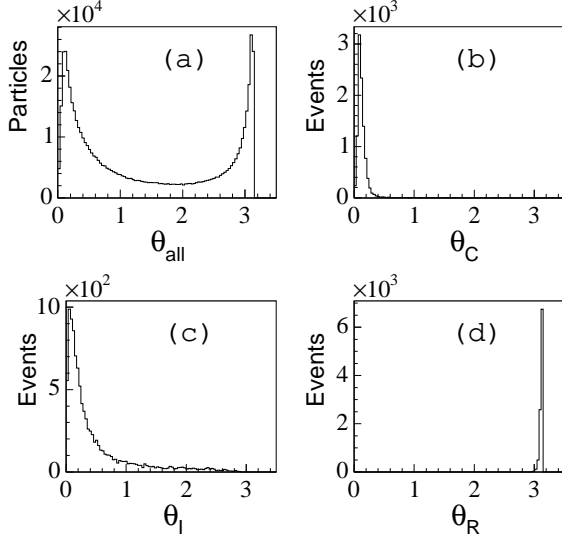


FIG. 3: The distribution of θ defined in hcm frame. (a) for all final state particles; (b) (c) (d) are calculated from the momenta of current quark, instanton part and proton remnant, respectively, at partonic level.

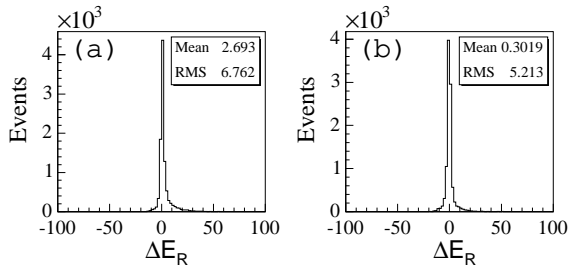


FIG. 4: The energy reconstruction errors of proton remnant by doing two cuts in θ in hcm(a) $\theta_{\text{cut}} = \frac{\pi}{2}$, (b) $\theta_{\text{cut}} = \frac{2\pi}{3}$. The legends show the Mean and RMS.

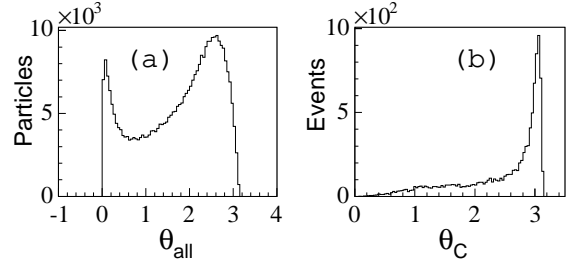


FIG. 5: θ distribution in cm2, (a) for final state particles (C+I), (b) for instanton before hadronization.

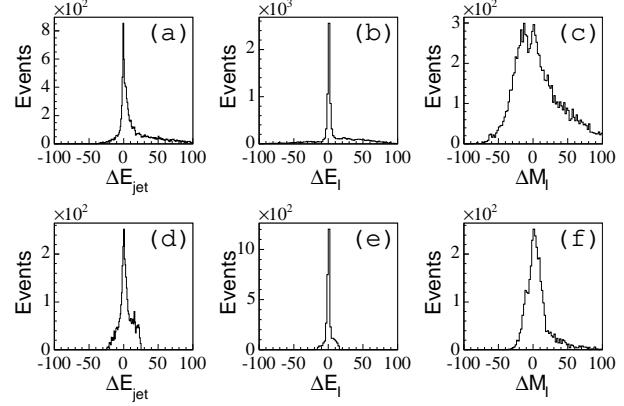


FIG. 6: The reconstruction errors for jet energy ΔE_{jet} , instanton energy ΔE_I and instanton mass ΔM_I in p_z -sorting method. Bottom panels are the results of a cut on $\Delta E < 10\%$ of top panels.

3(a), the peak around $\theta = \pi$ is narrower than that around $\theta = 0$. So, θ_{cut} should be in a place on the right of $\frac{\pi}{2}$. We find that $\theta_{\text{cut}} = \frac{2\pi}{3}$ is better than $\theta_{\text{cut}} = \frac{\pi}{2}$, which results in a better reconstruction of the energy of proton remnant, *cf.* Fig. 4.

We define the reconstruction error of a variable Y as the difference between the reconstructed value and the true value before hadronization, *i.e.*

$$\Delta Y = \frac{Y_{\text{rec}} - Y_0}{|Y_0|} \times 100\%, \quad (2)$$

where Y_{rec} represents the reconstructed value, Y_0 represents the true value before hadronization. In contrast to the case of $\theta_{\text{cut}} = \frac{\pi}{2}$ (see Fig. 4(a)), the energy reconstruction error for R after $\theta_{\text{cut}} = \frac{2\pi}{3}$ (see Fig. 4(b)) is focused at 0 and has a smaller RMS. In other words, the $\theta_{\text{cut}} = \frac{2\pi}{3}$ method reconstructs the energy of R more precisely.

After discarding R by doing $\theta_{\text{cut}} = \frac{2\pi}{3}$, the left particles are the mixture of C and I. Boost (C+I) to their c.m.s. frame (cm2 for short). Take the momentum direction of current quark, *i.e.* the direction of the jet axis, as the Z axis of cm2. The θ distribution of final state particles (C+I) in cm2 is shown in Fig. 5(a) and that of instanton before hadronization in Fig. 5(b). The two peaks in Fig. 5(a) represent current jet and IFS respectively. Since the Z axis is in the direction of jet axis, the peak around $\theta = 0$

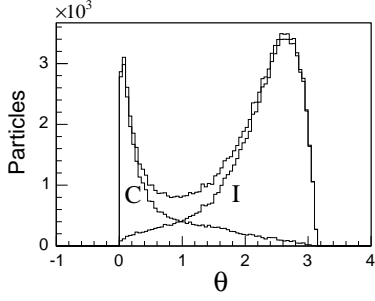


FIG. 7: The θ distribution in cm2 of identified C and I by p_z -sorting method.

represents the current jet particles, while the other peak, around $\theta = \pi$, represents the IFS.

Renumber these n particles by their p_z , sorting them according to $p_{z1} > p_{z2} > \dots > p_{zn}$. Accumulating the energy from particle 1 to particle k gives $E_k = \varepsilon_1 + \varepsilon_2 + \dots + \varepsilon_k$ (ε_i represents the energy of the i -th particle); simultaneously accumulating the energy from particle $k+1$ to n gives $E'_k = \varepsilon_{k+1} + \varepsilon_{k+2} + \dots + \varepsilon_n$. Taking particles from 1 to k as current jet, from $k+1$ to n as IFS, the energy reconstruction errors for jet and instanton are $\Delta E_{\text{jet}} = \frac{E_k - E_C}{E_C} \times 100\%$ and $\Delta E_I = \frac{E'_k - E_I}{E_I} \times 100\%$, respectively, where E_C is the energy of current parton, E_I is the energy of the quark and gluon included in IFS at partonic level. The value of the parameter k is chosen to make $\Delta E = 0.4 \times |\Delta E_{\text{jet}}| + 0.6 \times |\Delta E_I|$ minimum.

The reconstruction errors for the energy of jet, the energy of instanton and the mass of instanton are shown in Fig's. 6 (a), (b) and (c), respectively. It can be seen that large error events occur with some probability and the mass of instanton has not been reconstructed well. The criterion on which we judge for a good reconstruction quality is based on that the reconstruction error centralizes around 0 and has a narrow RMS. After doing a cut $\Delta E < 10\%$, both are improved — large error events have been cut out and the mass of instanton is reconstructed better at the expense of throwing away 67% of the events, *cf.* Fig's. 6 (d), (e), (f).

Up to now, the current jet and IFS are separated. The θ distribution of each part in cm2 are shown in Fig. 7. Jet particles centralize around $\theta = 0$, IFS centralizes around $\theta = \pi$. At intermediate θ the two parts overlap. They are separated by their p_z .

Method 2: 2D-cut

Based on the 2D plot shown in Fig. 2 and enlightened by the quadrant method (or quadrate-cut method) used in [14], an improved polygonal cut is used in η - ϕ -plane to isolate each part. Considering that the relative position of C and I in η - ϕ -plane strongly depends on the virtuality Q^2 of photon, the polygonal cut is running with Q^2 , as shown in Fig. 8. Using these cuts each part is identified. The reconstruction errors are shown in the upper panels of

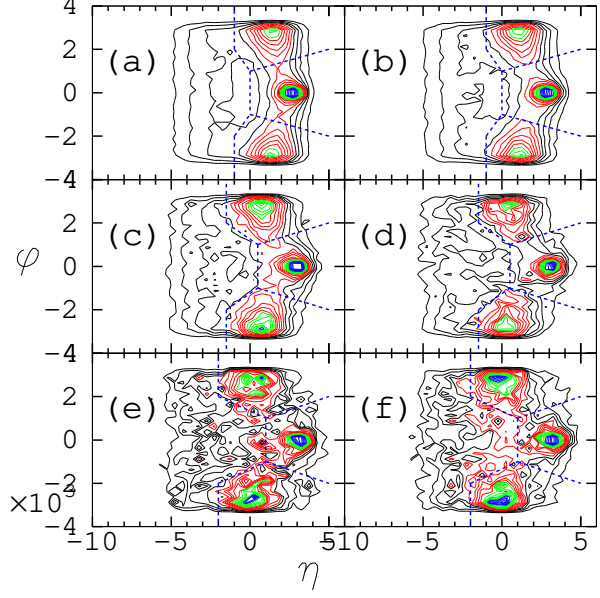


FIG. 8: (Color online) Running of the polygonal cuts (dashed lines) with Q^2 . The intervals of Q^2 for (a), (b), (c), (d), (e), (f) are [113, 200], [200, 400], [400, 600], [600, 800], [800, 1000], [1000, ∞] GeV^2 , respectively.

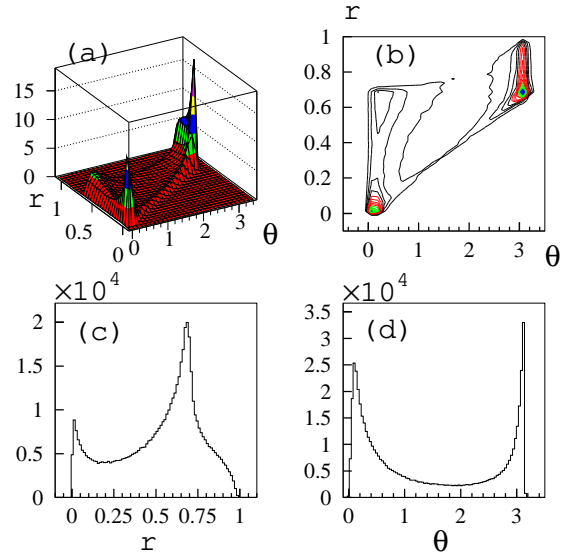


FIG. 9: (Color online) (a) (b) are 2D plots r vs. θ in hcm, surface and contour plots, respectively; (c) (d) are 1D distribution for r and θ respectively. All the variables are calculated in hcm.

Fig. 10.

Method 3: r -sorting in 2D plane

Comparing the two methods mentioned above it can be seen that the p_z -sorting method gives better reconstruction. However, it disregards totally the information contained in the θ - ϕ -plane, *cf.* Fig. 2, which has been taken into account in the 2D-cut

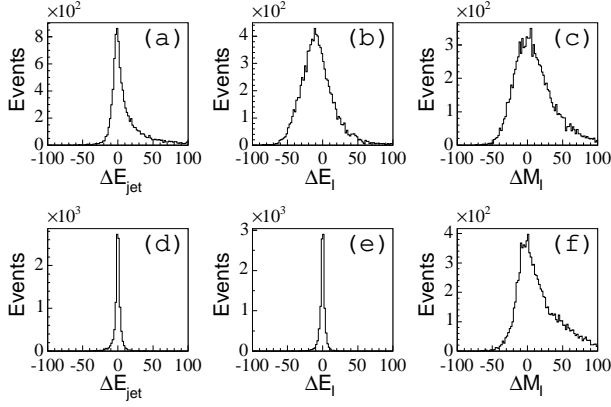


FIG. 10: The reconstruction errors for jet energy ΔE_{jet} , instanton energy ΔE_I and instanton mass ΔM_I in 2D-cut method (upper panels). Shown in the bottom panels are the results of r -sorting method.

method. Therefore, we try to combine the two methods.

Let us define a distance in θ - ϕ -plane,

$$r(\theta, \phi) = \sqrt{\frac{(\frac{\theta-\theta_0}{\pi})^2 + (\frac{\phi-\phi_0}{\pi})^2}{2}}, \quad (3)$$

where (θ_0, ϕ_0) is the position of current quark. This variable measures how far every final state particle is from the jet axis. Choosing an appropriate value for r_0 the particles with $r(\theta, \phi) < r_0$ are attributed to jet. The distribution of $r(\theta, \phi)$ is plotted in Fig. 9.

First discard R by 1D cut $\theta^{\text{hcm}} > \frac{2\pi}{3}$. Renumber the left n particles by their r , let $r_1 < r_2 < \dots < r_n$. Accumulating the energy from particle 1 to particle k gives $E_k = \varepsilon_1 + \varepsilon_2 + \dots + \varepsilon_k$, simultaneously accumulating energy from $k+1$ to n gives $E'_k = \varepsilon_{k+1} + \varepsilon_{k+2} + \dots + \varepsilon_n$. Taking particles from 1 to k as current jet, from $k+1$ to n as IFS. The value of r_0 is chosen to optimize the energy reconstruction, *i.e.* make $\Delta E = 0.4 \times |\Delta E_{\text{jet}}| + 0.6 \times |\Delta E_I|$ the minimum. The reconstruction errors are shown in Fig's. 10 (d), (e) and (f).

It is obvious that r -sorting in 2D plane gives the best reconstruction among the 3 methods described above.

IV. A COMPARISON OF THE ISOTROPY DEGREE OF IFS AND JET

IFS are expected to be isotropically distributed in its rest frame. Jet fragments are anisotropy, being axially symmetric. To quantify the degree of isotropy we use the sphericity.

Sphericity is a measure of how isotropically a collection of 4-momenta is distributed in three dimensions. A normalized momentum tensor is calculated from the momenta of the particles in consideration,

i.e.

$$S^{\alpha, \beta} = \frac{\sum_i P_i^\alpha P_i^\beta}{\sum_i |P_i|^2}, \quad (4)$$

where $\alpha, \beta=1, 2, 3$ correspond to the x, y and z components. By standard diagonalization of $S^{\alpha, \beta}$ one find three eigenvalues $\lambda_1 \geq \lambda_2 \geq \lambda_3$, with $\lambda_1 + \lambda_2 + \lambda_3 = 1$. The sphericity of the event is then defined as

$$S = \frac{3}{2}(\lambda_2 + \lambda_3). \quad (5)$$

An ideally isotropic system with infinite multiplicity has $S = 1$, while a perfectly anisotropic system has $S = 0$.

For a comparison, the sphericity of IFS and current jet in their own rest frames identified by the above-mentioned r -sorting method are calculated and the corresponding sphericity distributions are shown in Fig's. 11 (a) and (b), respectively. The mean values are

$$\bar{S}_{\text{IFS}} = 0.53 \pm 0.18, \quad \bar{S}_{\text{jet}} = 0.20 \pm 0.17. \quad (6)$$

Since the value of sphericity depends on multiplicity, we constructed an ideal sample, which has the same multiplicity as the IFS sample but has ideally isotropic momentum distribution for every event, *i.e.* using the thermalized momentum distribution, Eq. (7) below, for each component. The resulting sphericity is drawn in Fig's. 11 (a) as dashed line. The corresponding Mean is $\bar{S}^{\text{idea}} = 0.78 \pm 0.09$. The mean sphericity for IFS nearly equal to the ideally isotropic value means that IFS is approximately isotropic in its rest frame. The jet is destined to get low value of sphericity for its axial symmetry.

In view of the approximate isotropy of IFS we plot the distribution of the three momentum components p_x, p_y, p_z of IFS in its c.m. frame as shown in Fig. 12 (a). They coincide approximately. The distribution of the average \bar{p}_i of these three components is shown in Fig. 12 (b).

For a thermalized system the momentum component distribution is

$$dP(p_i) = \frac{1}{\sqrt{2\pi m k_B T}} e^{-p_i^2 / (2m k_B T)} dp_i, \quad i = x, y, z. \quad (7)$$

Fitting the \bar{p}_i distribution shown in Fig. 12 (b) to this formula we get the “temperature” of IFS as

$$\begin{aligned} T &= 863.86 \text{ MeV for } m = m^\pi, \\ &= 244.22 \text{ MeV for } m = m^K, \\ &= 128.50 \text{ MeV for } m = m^p. \end{aligned} \quad (8)$$

This “temperature” is actually not a thermal one, since at such high temperature there will be deconfinement and no hadron can survive.

The “temperature” T in Eq's. (8) is a parameter characterizing the phase-space distribution of particles in IFS. Its high value means that the quark-gluon fusion in the presence of instanton is a very hard process.

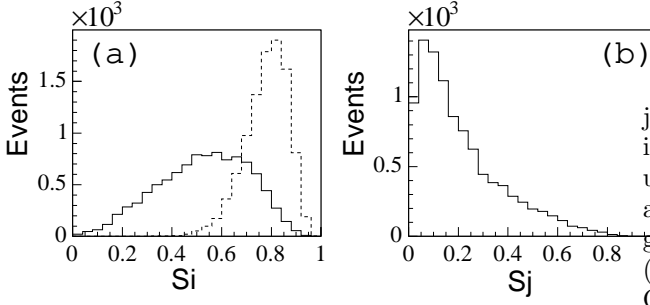


FIG. 11: Sphericity for IFS (a) and current jet (b) in their respective rest frame. Dashed line in (a) shows the sphericity for a ideally isotropic model with the same multiplicity as the IFS sample.

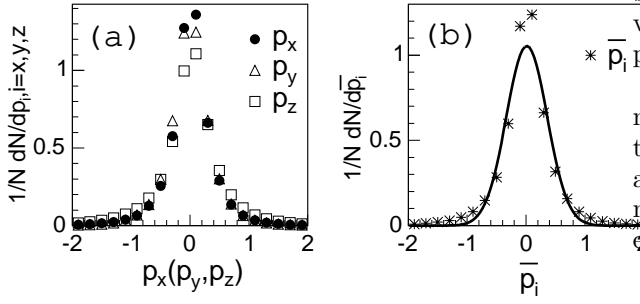


FIG. 12: (a) Momentum-component distribution of IFS in its rest frame; (b) the distribution of the mean value of the three components, fitted to thermalized momentum distribution.

V. SUMMARY

The identification of instanton final state, current jet and proton remnant in instanton induced deep inelastic scattering is studied using Monte Carlo simulation. Different methods — p_z -sorting, 2D-cut and r -sorting, for the reconstruction of the quark-gluon fusion product in the background of instanton (IFS) and current jet are tried and compared using QCDINS Monte Carlo event generator. A method to optimize the energy reconstruction is applied, which can reconstruct well the energies of current jet and instanton as well as the mass of the latter. It is found that r -sorting method gives the best reconstruction.

The sphericities of IFS and current jet identified by the r -sorting method are calculated. The high value of sphericity for IFS means that IFS is approximately isotropic in its rest frame.

The momentum distribution of IFS approximately mimics a thermalized distribution. The “temperature” fitted is rather high, which can be taken as a characteristic parameter for measuring the “hardness” of the quark gluon fusion process in the presence of instanton.

Acknowledgement This work is supported by National Natural Science Foundation of China under project 10475030 and 10375025 as well as the Cultivation Fund of the Key Scientific and Technical Innovation Project Ministry of Education of China NO CFKSTIP-704035. One of the authors, Xu Mingmei, thanks B. B. Levchenko for enlightening discussion.

-
- [1] A. Belavin, A. Polyakov, A. Schwartz and Yu. Tyupkin, Phys. Lett. B **59**, 85 (1975).
 - [2] G. 't Hooft, Phys. Rev. Lett. **37**, 8 (1976).
 - [3] G. 't Hooft, Phys. Rev. D **14**, 3432 (1976); Erratum in Phys. Rev. D **18**, 2199 (1978).
 - [4] G. 't Hooft, Phys. Rep. **142**, 357 (1986).
 - [5] S. Moch, A. Ringwald and F. Schrempp, Nucl. Phys. B **507**, 134 (1997).
 - [6] A. Ringwald and F. Schrempp, Phys. Lett. B **438**, 217 (1998).
 - [7] A. Ringwald and F. Schrempp, Phys. Lett. B **459**, 249 (1999).
 - [8] A. Ringwald and F. Schrempp, Proc. 8th Int. Seminar, Vladimir, Russia, 1994, D. Grigoriev et al. (eds.), p. 170. World Scientific, Singapore (1995) [hep-ph/9411217].
 - [9] The H1 Coll., Eur. Phys. J. C **25**, 495-509 (2002).
 - [10] J. Gerigk, Dipl. Thesis, University of Hamburg and MPI-PhE/98-20 (Nov. 1998), also at http://www-h1.desy.de/publications/theses_list.html.
 - [11] B. Koblitz, J. Phys. G: Nucl. Part. Phys. **28** 927-938 (2002).
 - [12] T. Carli, J. Gerigk, A. Ringwald and F. Schrempp, DESY 99-067, MPI-PhE/99-02, hep-ph/9906441.
 - [13] The ZEUS Coll., Eur. Phys. J. C **34**, 255-265 (2004).
 - [14] M. Sievers, PhD thesis, available on <http://www-library.desy.de/diss00.html>.
 - [15] S. Hillert, PhD Thesis, University of Hamberg, available on <http://www-library.desy.de/diss02.html>.
 - [16] A. Ringwald and F. Schrempp, Comput. Phys. Commun. **132**, 267 (2000) [hep-ph/9911516].
 - [17] M. Gibbs, A. Ringwald and F. Schrempp, in: Proc. DIS 1995 (Paris, France, 1995), J.-F. Laporte, Y. Sirois, Eds., pp. 341, hep-ph/9506392.
 - [18] G. Marchesini and B. Webber, Nucl. Phys. B **310**, 461 (1988).
 - [19] G. Marchesini et al., Comput. Phys. Commun. **67**, 465 (1992).